

## Crystal growth morphology of magnesium hydroxide

Jian-Song WU<sup>1,3,\*</sup>, Juan DU<sup>2</sup>, Yi-Min GAO<sup>1</sup>

<sup>1</sup>State Key Laboratory for Mechanical Behavior of Materials, Xi'an Jiaotong University, Xi'an, China

<sup>2</sup>Sino-European Institute of Aviation Engineering, Civil Aviation University of China, Tianjin, China

<sup>3</sup>School of Chemistry Science and Technology, Zhanjiang Normal College, Zhanjiang, China

Received: 05.09.2012 • Accepted: 07.10.2013 • Published Online: 14.04.2014 • Printed: 12.05.2014

**Abstract:** In this paper, the formation process of magnesium hydroxide unit cells, as well as the structural characteristics and growth morphology of magnesium hydroxide, is discussed from the perspective of growth units. The growth process of the hexagonal structure of the magnesium hydroxide is as follows: the growth units are first incorporated into a larger hexagonal dimension unit on the same plane, and then the hexagonal layers connect to each other in the z-axis direction for the hexagonal magnesium hydroxide unit cell. The results of the study show that the model of anion coordination polyhedron growth units may be reasonably deduced by using the unit cell structure and growth mechanism of magnesium hydroxide. After using Raman spectroscopy of the magnesium hydroxide growth solution Raman shift, the growth units of the magnesium hydroxide are shown to be octahedral:  $[Mg - (OH)_6]^{4-}$ .

**Key words:** Model of anion coordination polyhedron growth units, magnesium hydroxide, growth morphology, whisker

### 1. Introduction

Magnesium hydroxide is an important class of inorganic functional material. The hexagonal structure of magnesium hydroxide is an excellent inorganic flame retardant, as its whiskers possess strong reinforcement and toughening functions. Magnesium hydroxide has potential applications in various fields, due to the fact that it is capable of greatly increasing the strength, rigidity, dimensional stability, and deformation temperature of plastic.<sup>1,2</sup> Previous studies have reported on the development and application of magnesium hydroxide whiskers. However, recent research concerning magnesium hydroxide whiskers has not provided reasonable explanations for the following problems: first, what is the unit cell structure of magnesium hydroxide whiskers? How do the unit cells form? The most basic question that requires understanding is how the whiskers initiate and grow, which is also the basic issue that research regarding magnesium hydroxide whiskers must address. Second, why do magnesium hydroxide whiskers belong to the hexagonal crystal system? Their structure is octahedral, but at the same time does it also contain layers of compound? Why is its sphere accumulation categorized as “distorted hexagonal close packing”? Why does the slip phenomenon exist between the layers? Among the composites of magnesium hydroxide, why does the intercalated phenomenon exist between the layers? Third, why does magnesium hydroxide in different conditions form shapes with great division between them? What are the growth morphology and growth mechanism of magnesium hydroxide? Related studies have yet to address these core problems.

The research and application of crystal materials must focus on investigating the microcosmic growth

\*Correspondence: wujs1976@yahoo.com.cn

morphology and growth mechanism of such materials. In this paper, the growth mechanism, structure characteristics, and growth morphology of magnesium hydroxide unit cells are discussed, based on the model of anion coordination polyhedron (ACP) growth units proposed by Zhong and Shi et al.<sup>3-6</sup> The above-mentioned core problems of research regarding magnesium hydroxide may be logically answered based on the theoretical model of ACP growth units. It is not possible to do so by using the theoretical interface growth mechanism, PBC theory, etc. The theoretical model of ACP is capable of solving the growth mechanism and growth morphology of crystals at the microcosmic level, and, in essence, the ACP model not only emphasizes the determined action of the intrinsic lattice structures of crystals during crystal growth processes, but it also smoothly connects growth regulations with actual growth conditions. The ACP model has opened up a new method of studying crystal growth theory, and its application has achieved considerable achievements.<sup>7-16</sup>

## 2. Magnesium hydroxide crystal growth morphology

### 2.1. Structure and growth units of magnesium hydroxide crystals

The instruments for phase and Raman analyses were as follows. For X-ray diffraction (XRD), a D/Max-3C diffractometer (Rigaku, copper target, graphite curved crystal monochromator) set at a scanning rate of  $3^\circ \text{ min}^{-1}$  and scan range of  $10\text{--}70^\circ$  was used. An RM2000 confocal microprobe Raman spectroscope (Renishaw Company, UK) was used for Raman analysis.

According to the records of International Powder Standards (JCP2-07-0239), magnesium hydroxide crystal belongs to the hexagonal crystal system, the space group belongs to  $P3m1$ , its cell parameters are  $a = 0.314 \text{ nm}$  and  $c = 0.4769 \text{ nm}$ , and the particles of hexagonal flake magnesium hydroxide should possess a hexagonal crystal structure in SEM images. In order to perform research concerning the growth morphology of magnesium hydroxide, the following experiments are performed: using commercial and analytical grade  $\text{MgCl}_2 \cdot 6\text{H}_2\text{O}$  as the materials and sodium hydroxide as the precipitator,  $100 \text{ mL } 0.5 \text{ mol L}^{-1} \text{ MgCl}_2 \cdot 6\text{H}_2\text{O}$  and  $1.0 \text{ mol L}^{-1} \text{ NaOH}$  solutions are mixed; after mixing, the solutions are monitored using Raman spectroscopy. The  $1500\text{-mL}$  mixed solution is then transferred into a  $2\text{-L}$  autoclave, with a hydrothermal reaction temperature of  $T = 180^\circ \text{C}$  and a reaction time of  $t = 4 \text{ h}$ . After these steps are performed, the samples may be obtained. The TEM images of basic magnesium hydroxide are shown in Figure 1, showing among the crystal faces that are likely to appear (crystal face (0001)). Some of the particles possess an approximately hexagonal structure, such as the particle marked A in Figure 1, but some of the particles do not have standard hexagonal structures, such as the particle marked B in Figure 1. Some of the particles are circular, such as the particle marked C in Figure 1. The reasons for these shapes of particles are analyzed below. The phase of the synthesized samples was identified by XRD characterization, and the XRD patterns of the samples are shown in Figure 2. Compared with the diffraction standard (JCP2-07-0239), it is proven that the samples are indeed composed of magnesium hydroxide, and the XRD diffraction data of the crystal faces (001) and (110) are listed in the Table.

$d(001)$  and  $d_{(110)}$  may be calculated according to Bragg's law:  $2d\sin\Theta = \lambda$ . According to the structure of hexagonal crystal systems, indexing the data of diffraction gives us  $a = 0.3148 \text{ nm}$  and  $c = 0.4767 \text{ nm}$ . These data coincide very well with the data of the standard (JCP2-07-0239) record, proving that the samples are indeed composed of standard magnesium hydroxide crystals.

The Raman spectroscopy of the mixed solution was monitored, then mapped, and the results are displayed in Figure 3. Figure 3 shows that sharp peaks are located at  $694 \text{ cm}^{-1}$ ,  $823 \text{ cm}^{-1}$ ,  $1137 \text{ cm}^{-1}$ ,  $1008 \text{ cm}^{-1}$ ,  $1192 \text{ cm}^{-1}$ ,  $1332 \text{ cm}^{-1}$ ,  $1519 \text{ cm}^{-1}$ , and  $1733 \text{ cm}^{-1}$ , based on a normal vibrational Raman

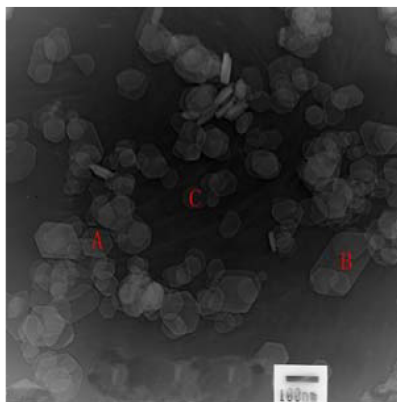


**Figure 1.** TEM images of hexagonal flake magnesium hydroxide.

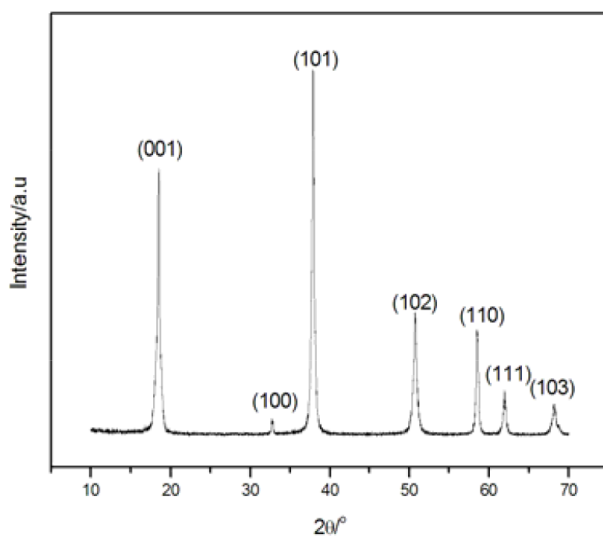


**Figure 2.** XRD patterns of magnesium hydroxide.

**Table.** XRD data of the crystal faces (001) and (110).

(001)			(110)		
$2\theta/^\circ$	$d/nm$	$I_{mas}/cps$	$2\theta/^\circ$	$d/nm$	$I_{mas}/cps$
18.59	0.4767	8875	58.56	0.1574	3507

active medium, polarization grade, Raman fermi resonance peak split, and a combination with computational chemistry.<sup>17,18</sup> These 8 peaks may be attributed to an anion coordination tetrahedron  $[Mg - (OH)_6]^{4-}$ . However,  $[Mg - (OH)_6]^{4-}$  is not octahedral, and its structure is shown in Figure 4. Mg is located in the octahedral center, and 6 hydroxyls are located in the 4 vertices of the octahedron; the angles in the crystal face of the 4 hydroxyl groups mutually form  $120^\circ$  (or  $60^\circ$ ) in the upper and lower sides of the crystal face, with the hydroxyls perpendicular to each other. In magnesium hydroxide crystal growth systems, the growth units of octahedral magnesium hydroxide crystals pile up and form magnesium hydroxide crystal unit cells based on certain rules. These large dimension growth units grow to be magnesium hydroxide crystals from the 3-dimensional direction, and this phenomenon is discussed in detail below.

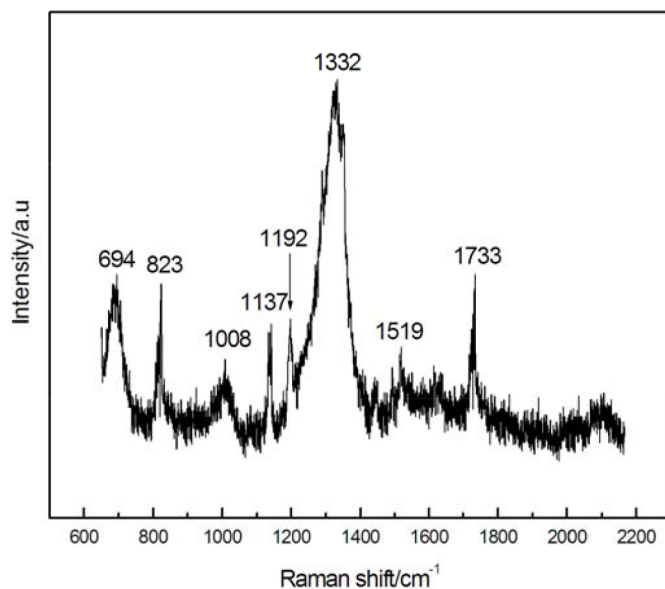


Figure 3. Raman shifts of magnesium hydroxide crystal growth solution.

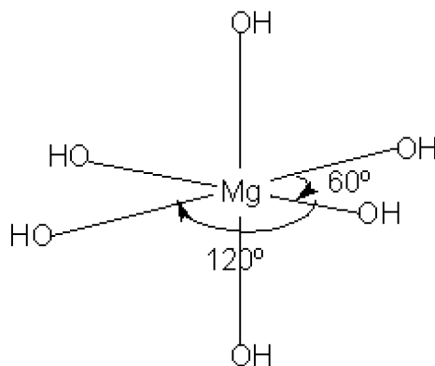
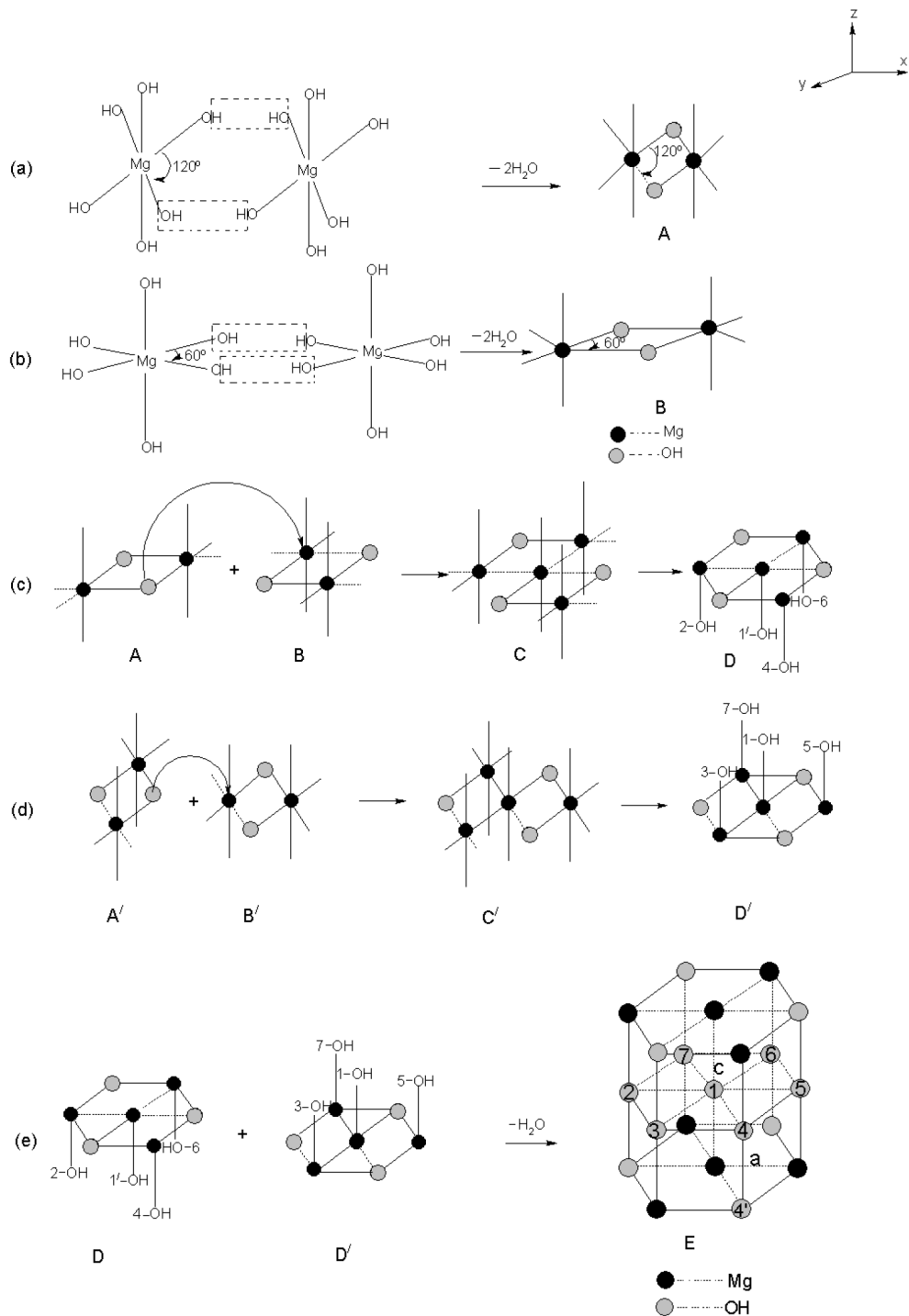


Figure 4. Hydrotalcite structure of magnesium hydroxide crystals.

## 2.2. Formation of magnesium hydroxide crystals

With unit cells in the conditions mentioned above, growth units  $[Mg - (OH)_6]^{4-}$  begin to pile up mutually; the pile up process is shown in Figure 5, and it may be seen that the growth units first pile up mutually at the same face. This pile up process is divided into 2 cases, the first of which is growth units that contain 2 hydroxides, and the angles of which mutually form  $120^\circ$  pile up with other growth units that contain 2 hydroxides with angles mutually forming  $120^\circ$  through the mutual dehydration of 2 hydroxides. Due to the fact that the electron negativity of oxidization is stronger, it is capable of attracting a proton  $H^+$  after the dehydration of 2 hydroxyl groups, and finally becomes a virtual “hydroxyl group” (i.e.  $-O^{\overset{H^+}{-}}$ ); therefore, we may consider the oxygen that is left behind after combining to be a virtual hydroxide. Now we can obtain a larger growth unit A by piling up the 2 growth units. In the A structure, the bond angle between the virtual hydroxide and magnesium (the angular vertex of which is magnesium, i.e.  $-O^{\overset{H^+}{-}} - Mg - O^{\overset{H^+}{-}}$ ) is  $120^\circ$ . When the angular vertex is virtual hydroxide ( $Mg - O^{\overset{H^+}{-}} - Mg$ ), then the bond angle is  $60^\circ$ ; this process is shown

in Figure 5(a). The other case involves growth units that contain 2 hydroxides, the angles of which mutually form a  $60^\circ$  pile up with other growth units that contain the 2 hydroxides the angle of which mutually forms  $60^\circ$  through the mutual dehydration of 2 hydroxides, and virtual hydroxide is also left behind after combining. Now we may also obtain a larger growth unit B by piling up the 2 growth units. In the B structure, the bone



**Figure 5.** The incorporation process of growth units and the formation process of magnesium hydroxide unit cells.

angle of  $-O^{H^+} - Mg - O^{H^+}$  is  $60^\circ$  and that of  $Mg - O^{H^+} - Mg$  is  $120^\circ$ ; this process is shown in Figure 5(b). After producing A and B, the 2 begin to pile up with each other. This type of combination is also divided into 2 cases, in the first of which an A pile is assumed with a B pile up along the direction of the Y axis (diagonal line consisting of O and O originating from a coincidence or parallel with the direction of the Y axis, a diagonal line consisting of Mg and Mg B originating from a coincidence or parallel with the direction of the Y axis); then we may determine C. The result of piling up A and B is one of virtual hydroxide  $-O^{H^+}$  forming A replaced by Mg from B. The pile up process is as follows: due to the fact that the angle of  $Mg - O^{H^+} - Mg$  from A is  $120^\circ$  when A relatively collides with B along the direction of the Y axis, the 2 free hydroxyls form B in parallel, and collide with the 2 sides of the angle of  $Mg - O^{H^+} - Mg$ ; then the bone of  $Mg - O^{H^+} - Mg$  reopens during the collision of the units, which affects with  $H_2O$ , causing it to be reduced to 2 free hydroxyls. These 2 free hydroxyls of A must relatively collide with the other 2 free hydroxyls of B in parallel, so that the 4 hydroxyls are not only parallel to each other, but they also collide with each other. The repulsion between the negative charges is large, as is the potential energy; therefore the hydroxyls are forced to either disappear directly, or to combine with  $H^+$  and become  $H_2O$  and then disappear, decreasing the potential energy of the system. At this time, the Mg from A is directly connected with that from B, and therefore C may be obtained. In order to produce a chart conveniently, the authors simply recorded free hydroxyls from the direction of the z axis in C, and provided marks to note them. The free hydroxyls that originated from the other directions were not recorded. At this time D was obtained, the process for which is shown in Figure 5(c); the second case assumes that one of the A' piles up with one of the B' along the direction of the X axis (diagonal line consisting of O and O originating from the A' coincident or parallel with the direction of the X axis, diagonal line consisting of Mg and Mg B' originating from the coincidence or parallel with the direction of the X axis); then C' may be determined, the piling up process for which is the same as in cases of A and B. Free hydroxyls from the positive direction of the Z (+Z) axis in C' are recorded and marks are made for them, and the free hydroxyls that originated from the other directions are not recorded; at this time D' is recorded, the process for which is shown in Figure 5(d). Finally, D is piled up with D' at the direction of the Z axis, and we are given magnesium hydroxide crystal unit cell E, the process for which is shown in Figure 5(e). During the process of piling up (e), the hydroxyl that is marked 1 in D piles up with the hydroxyl marked with 1' in D' by dehydration, and the other hydroxyls pile up with the other through hydrogen bonding. For example, in crystal unit cell E, the hydroxyl marked 4 piles up with virtual hydroxide  $-O^{H^+}$  that is marked 4' through hydrogen bonding. The question is why do only the hydroxyls of 1' and 1 pile up by dehydration and the others pile up with each other through hydrogen bonding? The reason for this is that both that the hydroxyls marked 1 and 1' are free hydroxyls; therefore their chemical activities are larger; however, the other hydroxyls are a different case, for example, the hydroxyls marked 4 are free hydroxyls ( $-OH$ ), but the hydroxyls marked 4' are virtual hydroxide  $-O^{H^+}$ ; of course, the chemical activity of virtual hydroxide is less than that of free hydroxyls; therefore, the former may only pile up through hydrogen bonding. The structural characteristics of magnesium hydroxide crystal unit cell E and the other characteristics produced due to structural characteristics will be discussed in the following section.

(i) Chemical formula of magnesium hydroxide crystal unit cells: In the structure of crystal unit cell E, E possesses 8 nodes located together with Mg. There are 4 nodes in each of the top and bottom faces, 4 nodes located at the face vertices, and 1 node located at the center of the faces. According to the hexagonal lattice

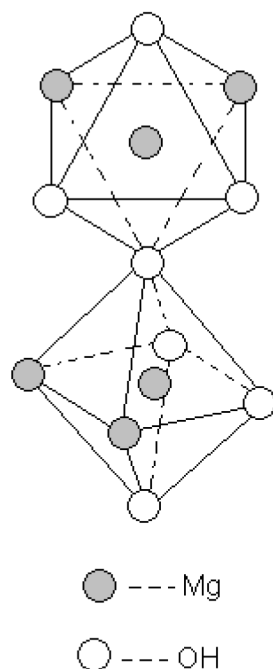


**Figure 6.** Positions of 2 octahedra in the c-axis.

node calculation, the Mg located at the face vertices only actually occupies  $\frac{1}{6}$  and the Mg located at the center of the faces only actually occupies  $\frac{1}{2}$ ; therefore, the actual total of Mg in a crystal unit cell is  $6 \times \frac{1}{6} + 2 \times \frac{1}{2} = 2$ . There are 3 nodes in the top and bottom faces of crystal unit cell E, all of which are located at the face vertices. Every edge possesses 1 hydroxyl, and the hydroxyls located at the edges only actually occupy  $\frac{1}{3}$ . One hydroxyl is located at the cube center. Therefore, the actual total of hydroxyls in a crystal unit cell is  $6 \times \frac{1}{6} + 6 \times \frac{1}{3} + 1 = 4$ , and the ratio of Mg and hydroxyl is 1:2, which corresponds to the formula of  $\text{Mg}(\text{OH})_2$ .

(ii) Symmetry of magnesium hydroxide crystal unit cells, octahedral structure, twisted hcp: If Mg originating from the top face rotates  $120^\circ$  around the c axis and then reflects along the cube center, then it is possible to recover the Mg. Thus, there are 3 shafts in the crystal. Clearly, there is a symmetric face m in the direction of the a-axis, and its symmetry completely corresponds to space group  $P\bar{3}m1$ .<sup>19</sup> From the piling process shown in Figure 5, it is known that magnesium hydroxide crystals retain their octahedral structure after their growth units have piled up. Mg is located at the center of the octahedron, and the 4 nodes are located at the face, containing the a-axis in a square as the face. The octahedron is composed of the hydroxyl of the c-axis on both sides of the vertex under the surface. Actually, a unit cell contains 2 octahedral half-square pyramids. Figure 6 shows the position of the 2 octahedrons in the c-axis of magnesium hydroxide crystal unit cell E. Clearly, 2 octahedrons force each other into a  $90^\circ$  distortion. Therefore, magnesium hydroxide in the sphere stacking mode is known as a distorted hexagonal close packing.

(iii) Magnesium hydroxide layer structure and the property of slip: The hydroxyls marked 1–7 all remain at the same face in crystal E, as shown in Figure 5, forming a layer structure. This layer consists of hydroxyls; therefore it is known as the hydroxyl layer. The top and bottom faces of the structure of the hexagonal lattice are the same, composed of 4 Mgs and 3 hydroxyls, and magnesium ions account for the majority of the hydroxyl minority. Thus we can call this layer the magnesium or metal layer, which is distinguished from the hydroxyl layer. In the crystal structures of the magnesium hydroxide, the metal and hydroxyl layers appear alternately;

therefore it may be said that magnesium hydroxide is a layer compound. As mentioned above, for a magnesium hydroxide crystal unit cell, since there are 7 hydroxyls in the hydroxyl layer, only the hydroxyl in the center (marked 1) piles up by dehydration, and the others are piled up by hydrogen bonding; therefore, this layer structure is not firm. First, it may easily slide around or distort the c-axis; thus the crystal face (i.e. (0001) face) in the hydroxyl layer is called the sliding surface or slide face, sliding around the c-axis along the a-axis direction, which makes the magnesium hydroxide grain shape become quasi-circular under certain growth conditions. As the grain marked C in Figure 1, this point is quite similar to the concentric growth rings of  $\text{CdI}_2$  crystals, as researched by Zhong et al.<sup>20</sup> because the structure of  $\text{Mg}(\text{OH})_2$  is similar to that of  $\text{CdI}_2$ , both of them being layer compounds, belonging to the  $P\bar{3}m1$  space group and having sliding faces capable of easily producing sliding. Secondly, it is easy to insert another anion between the hydroxyl layers to form new functional materials and intercalated layered compounds,<sup>21</sup> which is further evidence that one side of the hydroxyl layer is piled up by weak hydrogen bonding, a regulative process. Therefore, the hydroxyl layer has a special significance in the growth of the crystals and application of the magnesium hydroxide compound.

### 2.3. Growth mechanism for the formation of hexagonal magnesium hydroxide

The magnesium hydroxide crystal unit cell E is projected along the c-axis, as shown in Figure 5, and extended by 2 cycles in the same face (x, y), producing Figure 7. Figure 7 shows one of the mesh structures of the magnesium hydroxide crystals.

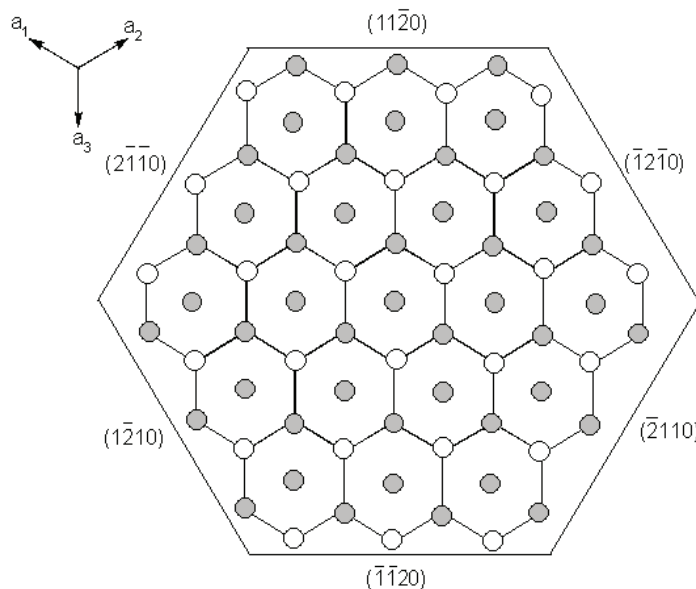


**Figure 7.** One of the mesh structures of the magnesium hydroxide crystals.

The following may be inferred from the composite process shown in Figure 5: on the outermost crystal faces of  $(2\bar{1}\bar{1}0)$ ,  $(\bar{1}2\bar{1}0)$ , and  $(\bar{1}\bar{1}20)$ , virtual hydroxyl ( $-\overset{H^+}{O}-$ ) is on the outermost surface, and  $\text{Mg}^{2+}$  is on the inside.  $\text{Mg}^{2+}$  is located inside the faces of the 6 lattices ( $(2\bar{1}\bar{1}0)$ ,  $(\bar{1}2\bar{1}0)$ , and  $(\bar{1}\bar{1}20)$ ), and, as a result, some virtual hydroxyl exits, which may be determined from the composite process shown in Figure 5. However, the crystal faces of  $(\bar{2}110)$ ,  $(\bar{1}2\bar{1}0)$ , and  $(11\bar{2}0)$  are the opposite of those of  $(2\bar{1}\bar{1}0)$ ,  $(\bar{1}2\bar{1}0)$ , and  $(\bar{1}\bar{1}20)$ , with  $\text{Mg}^{2+}$



on the outermost surface with 2 virtual hydroxyls, and  $(-O^{H+}-)$  relatively rearward within. According to the judgment rule of anion coordination polyhedron growth model of polar surface, the faces of  $(2\bar{1}\bar{1}0)$ ,  $(\bar{1}2\bar{1}0)$ , and  $(\bar{1}\bar{1}20)$  are negative polar faces, the crystal faces of  $(\bar{2}110)$ ,  $(\bar{1}2\bar{1}0)$ , and  $(11\bar{2}0)$  are positive polar faces, and the growth rate of the positive polar face is faster. This makes these 2 sets of crystal faces have different growth rates under certain conditions. There are more virtual hydroxyls in the positive polar faces of  $(\bar{2}110)$ ,  $(\bar{1}2\bar{1}0)$ , and  $(11\bar{2}0)$ ; therefore these positive polar faces will pile up at a higher growth rate in the system. There are only virtual hydroxyls in the crystal faces of  $(2\bar{1}\bar{1}0)$ ,  $(\bar{1}2\bar{1}0)$ , and  $(\bar{1}\bar{1}20)$ , and so these crystal faces are negative polar faces, which mainly depend on hydroxyl provided by growth units and are passive to incorporate. Therefore their growth rate is lower under certain conditions. For example, in the particle marked B in Figure 1, the crystal face of  $\{0001\}$  is not a regular hexagon; some of the side lengths are longer and some are shorter. The reason for the shorter side lengths is that they are located on positive faces, which grow more quickly. The reason for the longer side lengths is that they are located on negative faces, which grow more slowly, or that the crystal growth process is in essence the hydroxyl piling up process. Therefore, the number of hydroxyls directly determines the crystal growth rate, which means that it also directly determines the composite rate of the growth units in every crystal face. This may be determined from the model of XRD of magnesium hydroxide shown in Figure 2. Due to the fact that the fast growth rate of the crystal faces tends to disappear quickly, the crystal faces barely appear, their relative diffraction signal intensities of XRD are weak, and do not even appear in the diffraction peak. In contrast, the crystal faces that have slower growth rates appear easily; therefore their relative diffraction signal intensities of XRD are quite strong. To summarize, the growth process of magnesium hydroxide crystals is as follows: the growth units pile up with each other to form the large dimension growth units first in the same face (x, y), and these large dimension growth units are then connected to one another along the detection of the face of the  $\{0001\}$  (z-axis), and finally to the hexagonal structure of magnesium hydroxide. This point may also be easily determined from the XRD patterns shown in Figure 2. The relative diffraction signal intensity of the face  $\{0001\}$  is the second largest, the strongest face being that of the face (101). The question remains, why is the crystal face (001) diffraction front the strongest? The answer to this question may be observed from Figure 6. Each face  $\{0001\}$  has a (0001) crystal face diffraction, and there are 12 (101) crystal faces that are diffracted, revealing an area of 12 B crystal faces that is greater than that of the face (0001). Therefore, in the XRD standard of magnesium hydroxide, crystal face (101) is the strongest. If we were to obtain a majority grain of the regular hexagonal structure of the magnesium hydroxide during preparation, the alkali concentration would be increased, and the regular 6-party-like structure, the cross-section of which is parallel to the face of  $\{0001\}$ , is a regular hexagon or close in shape to a regular hexagon, such as the particle marked A in Figure 1. That is to say, the growth rate of units piling up with each other is the same or similar at the crystal faces of  $(2\bar{1}\bar{1}0)$ ,  $(\bar{1}2\bar{1}0)$ ,  $(\bar{1}\bar{1}20)$ ,  $(\bar{2}110)$ ,  $(\bar{1}2\bar{1}0)$ , and  $(11\bar{2}0)$ . It is easy to gain the same or a similar growth rate by increasing the alkali concentration during preparation. Research performed by Ye<sup>22</sup> shows that with a higher concentration of alkali (at least 4 moles) or a greater ration of alkali and magnesium ions (at least if  $C_{OH^-} : C_{Mg^{2+}} \geq 4 : 1$ ) we can obtain more regular structure unit particles of the magnesium hydroxide. How are such results possible? The reason is that the greater the concentration of alkali present, the more stable the growth unit octahedron  $[Mg - (OH)_6]^{4-}$  in the system will be, and it will possess a higher concentration, which will cause the growth rate of units piling up in the crystal faces of  $(2\bar{1}\bar{1}0)$ ,  $(\bar{1}2\bar{1}0)$ , and  $(\bar{1}\bar{1}20)$  to not be significantly different from those of  $(\bar{2}110)$ ,  $(\bar{1}2\bar{1}0)$ , and  $(11\bar{2}0)$ . This is regardless of whether active or passive incorporation is involved, because incorporation occurs on both sides, to large

dimension growth units, and when the concentration of the original primitive growth units  $[Mg - (OH)_6]^{4-}$  are large enough in the growing environment, they may eliminate the difference between the growth rate of active and passive piling up. Finally, the  $[Mg - (OH)_6]^{4-}$  of the incorporation rate in the crystal faces of  $(2\bar{1}\bar{1}0)$ ,  $(\bar{1}2\bar{1}0)$ ,  $(\bar{1}\bar{1}20)$ ,  $(\bar{2}110)$ ,  $(\bar{1}2\bar{1}0)$ , and  $(11\bar{2}0)$  is almost equal; thus the resulting lengths of the underside edges of the magnesium hydroxide hexagonal grain are equal, and then the grain becomes a regular structure. This is very consistent with the results reported by Wang et al.,<sup>23</sup> who performed research involving the ZnS crystal growth mechanism. Their study pointed out that when the solution alkalinity increased, the positive polar face growth rate gradually slowed down. In comparison with the negative polar face, the growth rate difference decreased, with the grain morphology changing from triangular to hexagonal. If the alkali concentration in the crystal growth of magnesium hydroxide system is exactly in line with or lower than the stoichiometry, then only pieces of grain and an uneven appearance may be obtained, and only part of the grain would be regular hexagonal, with a very small portion being round. A large number of other related experiments have also proven this point.

### 3. Conclusion

In this study, the cell structure of magnesium hydroxide is successfully derived using a model of anion coordination polyhedron growth units from the perspective of the growth units, and the results of the study are consistent with those of a large number of other studies. The growth process of the hexagonal-like magnesium hydroxide is as follows: octahedral growth units  $[Mg-(OH)_6]^{4-}$  are first incorporated into large-dimension hexagonal growth units on the same plane (x, y); then the large dimension hexagonal growth units are incorporated into magnesium hydroxide with a hexagonal prism structure on the z-axis. The optimum grain growth interface may then be predicted. Then it is combined with the structural features of large dimensions of growth units so that the growth of the crystals may be controlled.

### Acknowledgment

This work was supported by the National Natural Science Foundation of China, grant no. 51272207, China.

### References

1. Wu, J. S.; Xiao, Y. K.; Su, J. Y.; Deng, T. T.; Feng, J. R.; Zeng, M. *Sci. China Ser. E.* **2011**, *54*, 682–690.
2. Du, J.; Chen, Z.; Wu, Y. L.; Yang, M. D.; Dang J.; Yuan, J. J. *Turk. J. Chem.* **2013**, *37*, 228–238.
3. Shi, E. W.; Zhong, W. Z.; Hua, S. K.; Yuan, R. L.; Wang, B. G.; Xia, C. T.; Li, W. J. *Sci. China Ser. E.* **1998**, *28*, 37–45.
4. Zhong, W. Z.; Hua, S. K. *Morphology of Crystal Growth*, Science Press; Beijing, 1999.
5. Zhong, W. Z.; Liu, G. Z.; Shi, E. W.; Hua, S. K. *Sci. China Ser. B.* **1994**, *24*, 349–355.
6. Zhang, X. H.; Luo, H. S.; Zhong, W. Z. *Sci. China Ser. E.* **2004**, *34*, 241–253.
7. Shi, E. W.; Yuan, R. L.; Chen, Z. Z.; Zheng, Y. Q.; Tong, H. S.; Li, W.; Zhong, W. Z. *Sci. China Ser. E.* **2003**, *33*, 1–10.
8. Tian, M. Y.; Shi, E. W.; Yuan, R. L.; Wang, B. G.; Li, W. J.; Zhong, W. Z.; Zhuang, J. Y. *Sci. China Ser. E.* **1998**, *28*, 113–118.
9. Zhong, W. Z.; Yu, X. L.; Luo, H. S.; Cheng, Z. Q.; Hua, S. K. *Sci. China Ser. E.* **1998**, *28*, 320–324.
10. Wu, J. S.; Xiao, Y. K.; Wan, J. Y.; Wen, L. R. *Sci. China Ser. E.* **2012**, *55*, 872–878.

11. Shi, E. W.; Xia, C. T.; Wang, B. G.; Li, W. J.; Yuan, R. L.; Zhong, W. Z. *Sci. China Ser. E* **1997**, *27*, 126–133.
12. Zhong, W. Z.; Xia, C. T.; Shi, E. W.; Wang, B. G.; Li, W. J.; Hua, S. K. *Sci. China Ser. E* **1997**, *27*, 9–17.
13. Li, W. J.; Shi, E. W.; Tian, M. Y.; Wang, B. G.; Zhong, W. Z. *Sci Chin. Ser. E* **1998**, *28*, 212–219.
14. Zheng, Y. Q.; Shi, E. W.; Li, W. J.; Chen, Z. Z.; Zhong, W. Z. Hu, X. F. *Sci. China Ser. E* **2001**, *31*, 289–295.
15. Zheng, Y. Q.; Shi, E. W.; Li, W. J.; Chen, Z. Z.; Zhong, W. Z. Hu, X. F. *Sci. China Ser. E* **2001**, *31*, 204–212.
16. Chen, Z. Z.; Shi, E. W.; Yuan, R. L.; Zheng, Y. Q.; Li, W. J.; Zhao, T. R. *Sci. China Ser. E* **2003**, *33*, 589–596.
17. Xiang, S. F.; Ao, G. Q. *Medium Inorganic Chemistry*, Peking University Press, Beijing, 2003, pp. 25.
18. Liu, M. X.; Luo, G. A.; Zhang, X. Y.; Tong, A. J. *Instrument Analysis*, Tsinghua University Press; Beijing, 2002.
19. Du, P. Y.; Pan, Y. *Foundation of Material Science*, Chinese Building Materials Industry Press, Beijing, 2002, pp. 45.
20. Zhong, W. Z.; Hua, S. K. *Crystal Growth Morphology*, Science Press; Beijing, 1999, pp. 273–274.
21. Wu, J. S.; Xiao, Y. K.; Liu, Y. P.; Xu, W. B.; Lang, M. F.; Cheng, J.; Wan, J. P.; Chen, L. Z. *Turk. J. Chem.* **2011**, *35*, 881–891.
22. Ye, H. Master's degree paper of Shandong University, **2006**.
23. Wang, B. G.; Shi, E. W.; Zhong, W. Z. *Journal of Synthetic Crystals* **1997**, *26*, 189–189.